Immunity, Vol. 22, 329–341, March, 2005, Copyright ©2005 by Elsevier Inc. DOI 10.1016/j.immuni.2005.01.016

Regulatory T Cell Lineage Specification by the Forkhead Transcription Factor Foxp3

Jason D. Fontenot,[2,*] Jeffrey P. Rasmussen,[2] Luke M. Williams,[2] James L. Dooley,[2,3] Andrew G. Farr,[2,3] and Alexander Y. Rudensky[1,2,*]
[1]Howard Hughes Medical Institute
[2]Department of Immunology
[3]Department of Biological Structure
University of Washington
Seattle, Washington 98195

Summary

Regulatory T cell-mediated dominant tolerance has been demonstrated to play an important role in the prevention of autoimmunity. Here, we present data arguing that the forkhead transcription factor Foxp3 acts as the regulatory T cell lineage specification factor and mediator of the genetic mechanism of dominant tolerance. We show that expression of Foxp3 is highly restricted to the subset αβ of T cells and, irrespective of CD25 expression, correlates with suppressor activity. Induction of Foxp3 expression in nonregulatory T cells does not occur during pathogen-driven immune responses, and Foxp3 deficiency does not impact the functional responses of nonregulatory T cells. Furthermore, T cell-specific ablation of Foxp3 is sufficient to induce the identical early onset lymphoproliferative syndrome observed in Foxp3-deficient mice. Analysis of Foxp3 expression during thymic development suggests that this mechanism is not hard-wired but is dependent on TCR/MHC ligand interactions.

Introduction

Despite a large body of evidence demonstrating the functional properties of regulatory T cells (T_R) (Shevach, 2002), an unambiguous molecular definition of this cell type and its mechanism of action have yet to be realized. Due in large part to this problem, the very existence of T cells dedicated to maintaining self-tolerance was the source of great controversy until recently. A major breakthrough in the field came when a subset of $CD4^+$ T cells constitutively expressing the high-affinity IL-2 receptor alpha chain (CD25) was found to be highly enriched for immunosuppressive activity (Sakaguchi et al., 1995). While other molecules have been suggested to identify unique T_R cell populations, only the $CD4^+CD25^+$ T_R cell population has been consistently shown to display suppressive properties across species and in multiple disease models. Consistent with a role for these cells in maintaining self-tolerance, antibody depletion of $CD25^+$ cells in mice or reconstitution of lymphopenic mice with $CD25^-$ T cells results in the development of slowly progressing autoimmune inflammation in multiple organs. Nevertheless, the value of CD25 as a marker of the T_R cell population is limited. CD25 is highly expressed on both activated $CD4^+$ and $CD8^+$ T cells, obviating its utility in studying T_R cells in settings of immune activation.

The X chromosome-encoded forkhead transcription factor, Foxp3, was recently identified as a key player in $CD4^+CD25^+$ T_R cell biology. Unlike CD25, CTLA-4, GITR, and LAG-3 (markers proposed to define the T_R cell population), Foxp3 is not upregulated in recently activated $CD4^+CD25^-$ T cells. Consistent with a fundamental breakdown in self-tolerance, mice genetically deficient in Foxp3 succumb to a rapid and fatal lymphoproliferative autoimmune syndrome at 3–4 weeks of age (Brunkow et al., 2001; Fontenot et al., 2003; Godfrey et al., 1991). Moreover, Foxp3-deficient mice fail to generate a $CD4^+CD25^+$ T_R cell population (Fontenot et al., 2003). Ectopic expression of Foxp3 in nonregulatory T cells has been demonstrated to confer suppressor activity (Fontenot et al., 2003; Hori et al., 2003; Khattri et al., 2003). However, in these studies, only a subset of the Foxp3-expressing cells upregulated CD25 expression and acquired suppressor function after 2 weeks in vivo (Fontenot et al., 2003). Similarly, only those cells expressing the highest levels of Foxp3 acquired elevated levels of CD25 and were shown to possess suppressor activity in vitro (Hori et al., 2003). Together, these studies suggest that CD25 expression correlates more closely with suppressor activity than Foxp3 expression. Foxp3 has also been implicated in the cell intrinsic negative regulation of $CD4^+$ T cell activation (Clark et al., 1999; Khattri et al., 2001; Schubert et al., 2001). Furthermore, low levels of Foxp3 expression have been reported in $CD4^+CD25^-$ and $CD8^+$ T cells as well as in $B220^+$ cells (Brunkow et al., 2001; Fontenot et al., 2003; Hori et al., 2003) implying an as yet uncharacterized role in other hematopoeitc lineages. Thus, the role of Foxp3 in the hematopoietic system and the relationship between Foxp3, CD25 expression, and the T_R cell population has remained undefined.

The lack of an unambiguous molecular definition of T_R cells has severely hampered efforts to experimentally address the developmental processes that generate these cells and their functional role within the immune system. Given the much more aggressive autoimmune syndrome resulting from genetic deficiency in Foxp3 as compared to that resulting from $CD25^+$ T cell depletion, we hypothesized that Foxp3 expression would identify a T_R cell population beyond that defined by CD25 expression. Furthermore, we hypothesized that Foxp3 acts to establish and maintain a T_R cell genetic program and would thus be a definitive marker of the T_R cell population. To address these hypotheses, we have generated mice harboring a GFP-Foxp3 fusion protein-reporter knockin allele. Analysis of *Foxp3*^{gfp} mice demonstrates that Foxp3 expression identifies the T_R cell population. Our results argue that Foxp3 functions as the T_R cell lineage specification factor and mediator of the genetic mechanism of dominant tolerance.

*Correspondence: fontenot@u.washington.edu (J.D.F.); aruden@u.washington.edu (A.Y.R.)

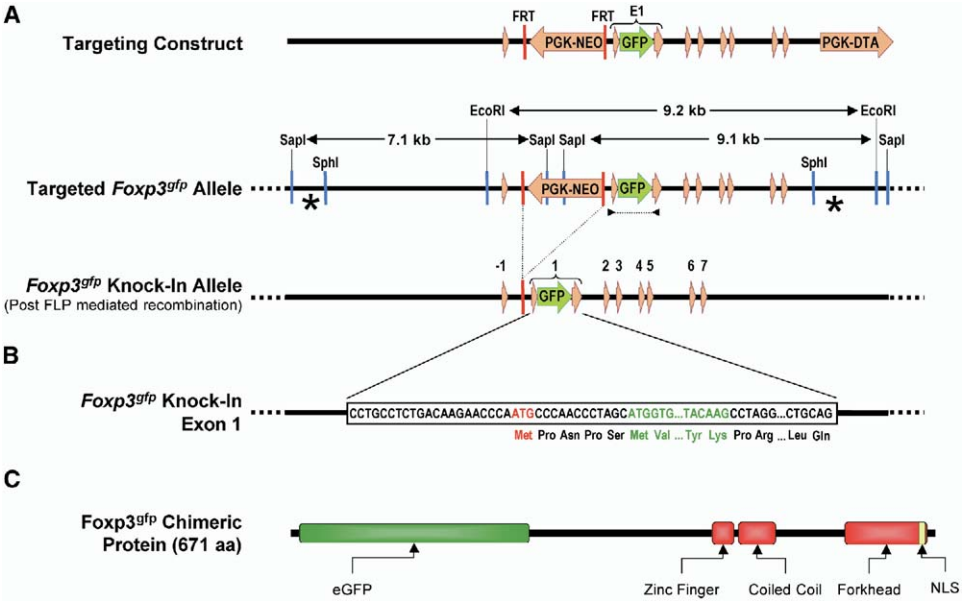

Figure 1. The *Foxp3*^{gfp} Allele

(A) Maps of the targeting construct and targeted *Foxp3*^{gfp} allele. Asterisks denote the location of external probes used for a Southern blot screen of ES cell clone DNA digested with the indicated restriction endonucleases. Black triangles denote oligonucleotide primers for PCR genotyping of the targeted allele.

(B) Enlarged view of the first coding exon of the *Foxp3*^{gfp} allele with the amino acid translation of the open reading frame below. The red "ATG" denotes the endogenous Foxp3 start codon. The green sequence denotes the eGFP-coding sequence.

(C) Scale diagram of the Foxp3^{gfp} chimeric protein.

Results

Generation and Characterization of the *Foxp3*^{gfp} Allele

To facilitate the analysis of Foxp3 expression at the single-cell level, we generated gene-targeted mice in which the complete eGFP coding sequence was inserted in-frame into the first coding exon of the *Foxp3* gene (Figures 1A and 1B and Figure S1; see the Supplemental Data available with this article online). The resulting allele (*Foxp3*^{gfp}) encodes a chimeric GFP-Foxp3 fusion protein (Foxp3^{gfp}), having eGFP inserted downstream of the first five N-terminal amino acids of Foxp3 and upstream of the entire remaining Foxp3 molecule (Figure 1C).

Only a single *Foxp3* allele is active in a given female cell due to random X chromosome inactivation (Schubert et al., 2001), and only a single allele is present in male cells. Thus, to be useful in studying the function of Foxp3, it was incumbent that the *Foxp3*^{gfp} allele faithfully recapitulate Foxp3 function. Consistent with this, male mice hemizygous for the *Foxp3*^{gfp} allele and homozygous *Foxp3*$^{gfp/gfp}$ female mice remained as healthy as their wild-type (wt) littermates throughout the period of observation (up to 9 months). Initial FACS analysis of *Foxp3*^{gfp} mice revealed a small, discrete population of GFP-expressing cells, confirming expression of the *Foxp3*^{gfp} allele (Figure 2A). Consistent with the nuclear localization of Foxp3, examination of individual GFP$^+$ cells with deconvolution microscopy revealed GFP expression almost exclusively within the nucleus (Figure 2B). FACS analysis showed that *Foxp3*^{gfp} and *Foxp3*^{wt} mice had equivalent percentages of all major lymphoid populations examined, including T cells and thymocytes (Figure S1).

Since, Foxp3 has been implicated in the thymic development of CD4$^+$CD25$^+$ T$_R$ cells, we next focused our analysis on this population. *Foxp3*^{gfp} mice had normal percentages of CD4$^+$CD25$^+$ T cells (Figure 2C), and these cells expressed characteristic patterns of multiple cell surface markers, including CTLA-4, GITR, and CD103 (Figure S1). Furthermore, in vitro functional analysis demonstrated that CD4$^+$CD25$^+$ T$_R$ cells from *Foxp3*^{gfp} and *Foxp3*^{wt} mice suppressed the proliferative response of wt CD4$^+$CD25$^-$ T cells with equal potency (Figure 2D). To test the competitive fitness of *Foxp3*^{gfp} versus *Foxp3*^{wt} CD4$^+$CD25$^+$ T$_R$ cells, we analyzed female mice heterozygous for the *Foxp3*^{gfp} allele. Because Foxp3 is required for development of the CD4$^+$CD25$^+$ T$_R$ cell population (Fontenot et al., 2003), random X chromosome inactivation predicts a 50:50 ratio of CD4$^+$CD25$^+$ T cells expressing either allele. Although there was significant variability from mouse to mouse, analysis of both CD4$^+$ SP thymocytes and peripheral CD4$^+$ T cells revealed an average ratio of ~1 between the proportions of GFP$^+$ to GFP$^-$ cells within the CD4$^+$CD25$^+$ T cell population (Figure 2E). These populations expressed identical patterns of the cell surface markers analyzed above (data not shown). Together, these results argue that the *Foxp3*^{gfp} allele fully recapitulates Foxp3 function.

Foxp3 Expression Identifies the T$_R$ Cell Population

To gain insight into the biological function of Foxp3 through its cell type-specific expression pattern, we an-

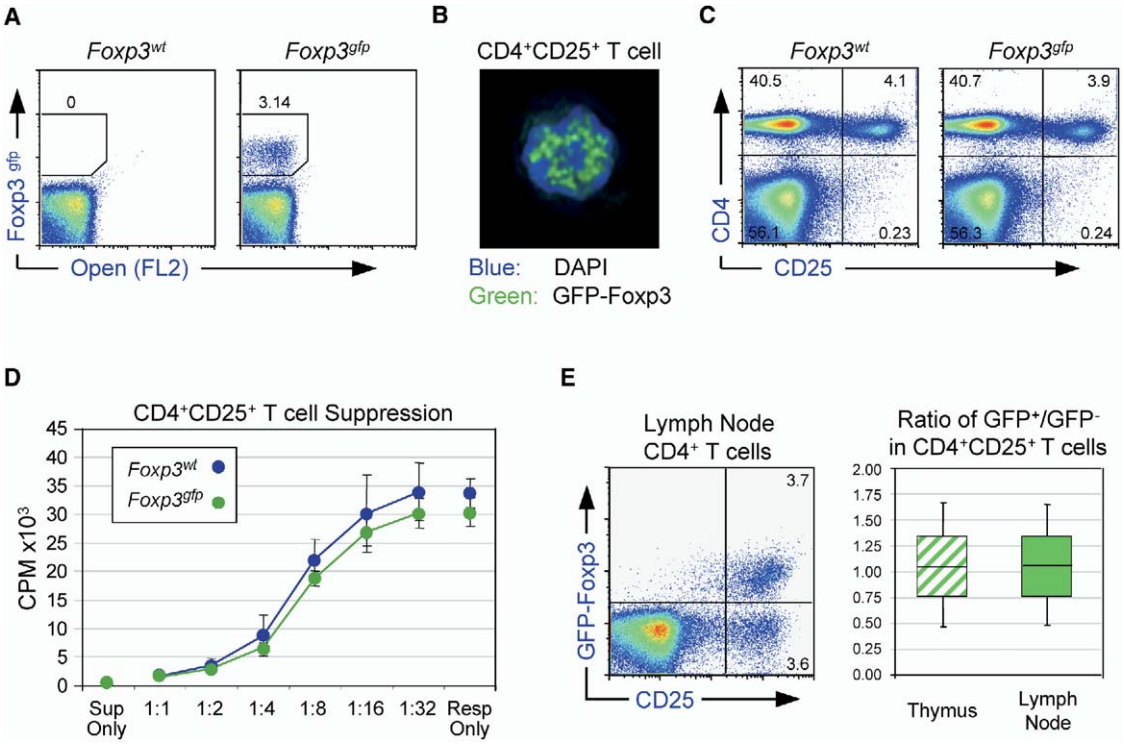

Figure 2. The *Foxp3*^{gfp} Allele Fully Recapitulates Wild-Type Foxp3 Function

(A) Expression of Foxp3^{gfp} in lymphocytes from *Foxp3*^{gfp} mice. Flow cytometric analysis of live gated lymph node cells from male littermates of the indicated genotype.

(B) Nuclear localization of Foxp3^{gfp}. Typical single-cell profile of purified CD4$^+$CD25$^+$ T cells from a *Foxp3*^{gfp} mouse that were counterstained with DAPI and analyzed by deconvolution microscopy.

(C) Analysis of CD4$^+$CD25$^+$ T cell subsets in *Foxp3*^{gfp} and *Foxp3*^{wt} mice. Flow cytometric analysis of live gated lymph node cells from littermate male mice of the indicated genotype.

(D) Comparable suppressor function of *Foxp3*^{gfp} and *Foxp3*^{wt} CD4$^+$CD25$^+$ T cells. An in vitro suppression assay was performed by using Con A stimulation of cocultures of 2 × 10^4 wt CD4$^+$CD25$^-$ T cells as responders, 8 × 10^4 irradiated *TCR*$\beta\delta^{-/-}$ splenocytes as APCs, and titrated numbers of CD4$^+$CD25$^+$ T cells from littermate male mice of the indicated genotype as suppressors. Data are presented as mean cpm ^{3}H-thymidine incorporation in triplicate cultures. Error bars indicate standard deviation of the mean.

(E) Analysis of *Foxp3*^{gfp} and *Foxp3*^{wt} CD4$^+$CD25$^+$ T cell subsets in female heterozygous *Foxp3*$^{gfp/wt}$ mice. Representative FACS analysis of CD4$^+$ cell gated lymph node cells from a female *Foxp3*$^{gfp/wt}$ mouse. The box plots show the average GFP$^+$/GFP$^-$ ratio among CD4$^+$CD25$^+$ cells as gated accompanying FACS plot from thymus and lymph node within the same animal (n = 10). Error bars indicate standard deviation of the mean.

alyzed Foxp3^{gfp} expression within the major hematopoietic lineages. Foxp3^{gfp} expression is highly restricted (>99.8%) to TCRβ^+ cells (Figure 3A). Lack of Foxp3^{gfp} expression in TCR$\gamma\delta^+$ and NK1.1$^+$ populations, which include both NK and NKT cells, further demonstrates that Foxp3 expression is limited to $\alpha\beta$ T cells. No Foxp3^{gfp} expression was observed in other hematopoietic lineages, including B cells, macrophages, and dendritic cells, either in unmanipulated mice or upon in vitro activation with immunostimulatory molecules including LPS, CpG DNA, and zymosan (data not shown). Consistent with these observations, FACS analysis of splenocytes, lymph node cells, and thymocytes from *RAG1*$^{-/-}$ *Foxp3*^{gfp} mice, which lack all T and B cells, revealed a complete loss of Foxp3^{gfp}-expressing cells (Figure 3B and data not shown). Furthermore, $\alpha\beta$ T cell-restricted expression of Foxp3 was maintained after infection of *Foxp3*^{gfp} mice with *Listeria monocytogenes* (L.m.), LCMV, or *Mycobacterium tuberculosis* (M.tb.) (data not shown). Thus, we conclude that, within the hematopoietic lineage, Foxp3 is uniquely expressed in $\alpha\beta$ T cells. To determine if Foxp3 was expressed in other nonhematopoietic cell types or tissues, we conducted immunohistochemical analysis of tissues from *RAG1*$^{-/-}$ *Foxp3*^{gfp} mice. Remarkably, no Foxp3 expression was detected in the thymus, secondary lymphoid organs, or nonlymphoid tissues, including brain, lung, liver, skin, and testes (data not shown).

Among lymph node cells, Foxp3 expression was largely restricted to CD4$^+$ T cells (>97% of Foxp3^{gfp+} cells are CD4$^+$CD8$^-$), but small populations of Foxp3-expressing TCRβ^+ cells expressed CD8, both CD4 and CD8 (DP), or neither CD4 nor CD8 (DN) (Figure 3C). No significant difference in Foxp3^{gfp} levels were observed among these four populations (data not shown). Distribution of Foxp3^{gfp+} T cells among the CD4/CD8 populations was similar in the lymph nodes, spleen, peripheral blood, bone marrow, and peripheral tissues, e.g., lung (data not shown). Since CD25 has been used as a marker for T_R cells, we next examined CD25 expression

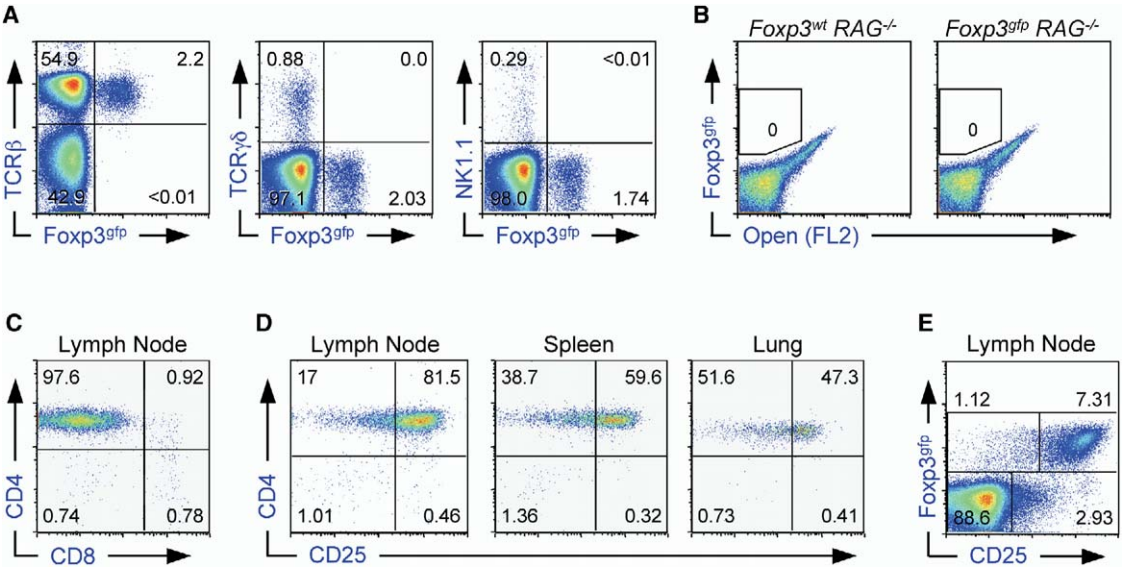

Figure 3. Foxp3 Expression Is Restricted to a Subset of αβ T Cells

(A) Foxp3 expression is restricted to TCRβ$^+$ cells. Flow cytometric analysis of Foxp3^{gfp} expression in live gated lymph node cells.

(B) Foxp3-expressing cells are lost in RAG-deficient mice. Flow cytometric analysis of live gated spleen cells from *RAG1*$^{-/-}$ mice of the indicated genotype.

(C) CD4 and CD8 expression among Foxp3-expressing cells. Flow cytometric analysis of lymph node cells from *Foxp3*^{gfp} mice; plot is gated on Foxp3^{gfp+} live cells.

(D) CD4 and CD25 expression among Foxp3-expressing cells. Representative flow cytometric analysis of Foxp3^{gfp+} cells from the indicated organ; cells within the live Foxp3^{gfp+} gate are shown.

(E) Foxp3 and CD25 expression in the CD4$^+$ T cell population. Flow cytometric analysis of lymph node cells within the live CD4$^+$ gate are shown.

within the total Foxp3^{gfp+} population. In healthy 6- to 8-week-old mice ~82% of lymph node Foxp3-expressing cells were CD4$^+$CD25^{hi} (Figure 3D). In the spleen the percentage of CD4$^+$CD25^{hi} Foxp3^{gfp+} T cells dropped to ~60% of Foxp3^{gfp+} cells. Remarkably, less than 50% of Foxp3^{gfp+} lymphocytes isolated from PBS-perfused lung expressed high levels of CD25. Thus, Foxp3^{gfp} expression is largely restricted to CD4$^+$ T cells, and a significant percentage of Foxp3^{gfp+} T cells express little or no CD25.

To address the relationship between Foxp3 and CD25 expression and T_R cell function, we next focused our analysis on the total CD4$^+$ T cell population. This population includes the vast majority (>97%) of Foxp3-expressing cells. Analysis of CD4$^+$ T cells revealed four populations: the CD25$^-$Foxp3^{gfp-} "naive" T cell subset, a population of CD25$^+$Foxp3^{gfp-} cells, CD25^{hi}Foxp3^{gfp+} cells, and a Foxp3^{gfp+} population expressing little or no CD25 (CD25^{lo}Foxp3^{gfp+}) (Figure 3E). The presence of both Foxp3^{gfp+} and Foxp3^{gfp-} CD25-expressing populations allowed us to directly address the relationship between CD25 expression and T_R cell function. To this end, the four indicated subpopulations of CD4$^+$ T cells (Figure 4A) were purified to >90% purity by using a combination of magnetic cell separation and FACS sorting. Functional analysis revealed that both populations of Foxp3^{gfp+} CD4$^+$ T cells were unresponsive to stimulation with ConA and APCs in vitro (Figure 4C). In contrast, the CD4$^+$CD25$^+$Foxp3^{gfp-} cells proliferated to a much greater extent than either the CD4$^+$CD25$^-$ Foxp3^{gfp-} or CD4$^+$ cells depleted of all Foxp3^{gfp+} cells. Finally, in vitro suppression assays revealed that both the CD4$^+$CD25^{hi}Foxp3^{gfp+} and CD4$^+$CD25^{lo}Foxp3^{gfp+} populations suppressed CD4$^+$ T cell proliferation with equal potency, while neither the CD4$^+$CD25$^-$Foxp3^{gfp-} cells nor the CD4$^+$CD25$^+$Foxp3^{gfp-} cells showed suppressor activity (Figure 4D). We conclude that Foxp3 expression, and not CD25 expression, directly correlates with T_R cell function.

Gene Expression Profiling of CD4 T Cell Subpopulations

To gain insight into the transcriptional program specified by Foxp3 expression, we interrogated the mRNA expression profiles of the four CD4$^+$ T cell subsets as defined by Foxp3^{gfp} and CD25 expression (Figure 4A) by using Affymetrix Mouse Genome 430 2.0 arrays. Normalized expression values from the "naive" CD4$^+$CD25$^-$Foxp3^{gfp-} population were used as a reference for pairwise comparison with values from each of the three "non-naive" populations. Genes with fold-changes meeting stringent selection criteria (see Experimental Procedures) were chosen, and these gene lists were analyzed for similarities and differences. Comparisons of the overlapping gene sets reveal that the two Foxp3-expressing populations (CD25^{hi} versus CD25^{lo}) share a largely common gene expression signature, whereas the CD25$^+$Foxp3^{gfp-} population exhibited little overlap with either of the Foxp3^{gfp+} populations (Figure 4E). In addition to very high levels of Foxp3

mRNA, both Foxp3^{gfp+} cell subsets displayed increased expression of IL-10, CD103, Klrg1, Nrp1, GITR, ICOS, Fgl2, Gpr83, and CTLA-4 and decreased expression of FasL, Sema4a, IL-4, Pde3b, and Pde7a (Figure 4F)—a gene expression pattern highly characteristic of T_R cells (Gavin et al., 2002; McHugh et al., 2002). These data demonstrate that both the CD25^{hi} and CD25^{lo} populations share a T_R cell gene expression profile and argue that Foxp3 expression specifies this transcriptional program.

Examination of the overlaps among these subpopulations reveals several other distinct gene expression patterns (Figure 4F). First, data sets from all three "nonnaive" populations share genes characteristic of activated lymphocytes (e.g., increased expression of OX40, CD44, IL2Rα/β, and hexokinase). Second, the CD25$^+$ Foxp3^{gfp-} cells show a gene expression profile characteristic of activated/effector T cells (increased expression of IL-2, IL-4, IL-17, T-bet, and Edg3, and decreased CD62L expression). FACS analysis of the CD25$^+$ Foxp3^{gfp-} population corroborates this analysis, showing a significant enrichment of cells with an activated phenotype—expressing high levels of CD69 and decreased levels of CD62L and CD45RB (Figure 4A). Finally, comparison of gene expression levels between the CD25^{lo} and CD25^{hi} Foxp3-expressing populations suggests that the CD25^{lo}Foxp3^{gfp+} population may be enriched for effector or tissue-homing cells (Figure 4F). Relative to the CD25^{hi} population, the CD25^{lo}Foxp3^{gfp+} cells have increased expression of ICOS, CCR2, CXCR3, CCR5, and β1-integrin. Again, FACS analysis reveals that this population is enriched for cells expressing high levels of CD69 and decreased levels of CD62L and CD45RB (Figure 4A). Consistent with these data, this subset is also significantly enriched for proliferating cells expressing Ki67, a cell cycle-associated nuclear protein (Figure 4B). These data are also in agreement with the enrichment of CD4$^+$CD25^{lo} Foxp3^{gfp+} T cells in the lungs of both uninfected and chronically M.tb.-infected mice (Figure 3C and data not shown).

No Cell Intrinsic Role for Foxp3 in Effector T Cell Function

The data presented thus far support the hypothesis that Foxp3 acts as the T_R cell lineage specification factor. However, increased proliferation and cytokine secretion by CD4$^+$ T cells isolated from Foxp3-deficient scurfy mice has led to the proposal that Foxp3 may also act as a cell-intrinsic negative regulator of CD4$^+$ T cell activation and inflammatory cytokine production (Clark et al., 1999; Khattri et al., 2001; Schubert et al., 2001). It has also been suggested that Foxp3-deficient CD4$^+$ T cells exhibit a decreased dependence on CD28-mediated costimulation (Clark et al., 1999). In fact, the ongoing lymphoproliferative syndrome in these mice complicates these conclusions. We sought to directly test whether Foxp3 deficiency can affect the dose dependence of, or costimulation requirements for, antigen-specific responses of naive nonregulatory CD4$^+$ T cells. To this end, we bred the *Foxp3*$^-$ allele onto OT-II TCR transgenic *RAG1*$^{-/-}$ mice. As reported, restricting the TCR repertoire to a single specificity for a known foreign antigen (in this case the ovalbumin 323–339 peptide, Ova) rescues Foxp3-deficient mice from the lymphoproliferative autoimmune syndrome (Zahorsky-Reeves and Wilkinson, 2001). OT-II *RAG1*$^{-/-}$*Foxp3*$^-$ mice were healthy and phenotypically indistinguishable from their OT-II *RAG1*$^{-/-}$*Foxp3*$^+$ littermates. Absolute numbers and relative percentages of thymocyte and peripheral T cell subpopulations in OT-II *RAG1*$^{-/-}$ *Foxp3*$^-$ and OT-II *RAG1*$^{-/-}$*Foxp3*$^+$ littermates were identical based upon expression of CD4, CD8, TCR, and a panel of additional cell surface markers (Figure S2). We conclude that Foxp3 deficiency does not impact the development of nonregulatory CD4$^+$ T cells. Importantly, mature T cells from OT-II *RAG1*$^{-/-}$*Foxp3*$^-$ mice showed no evidence of activation based upon expression levels of CD69, CD25, and CD62L (Figure S2). In this situation, we were able to directly compare the effect of Foxp3 deficiency on naive CD4$^+$ T cell function. OT-II *RAG1*$^{-/-}$ CD4$^+$ T cells from *Foxp3*$^-$ and *Foxp3*$^+$ mice mounted identical proliferative response to titrated amounts of the cognate Ova peptide in the presence of wt APCs and similarly diminished responses in the presence of costimulation-deficient APCs from *CD80/CD86* double knockout mice (Figure 5A). These results argue that Foxp3 deficiency does not impact the antigen sensitivity, costimulation requirement, or proliferative capacity of nonregulatory CD4$^+$ T cells.

To address the role of Foxp3 in a polyclonal nonregulatory T cell population exposed to more physiological immune stimuli, i.e. infection, we generated mixed bone marrow chimeras by transferring *Foxp3*$^-$ CD45.1$^-$ and *Foxp3*$^+$ CD45.1$^+$ congenic bone marrow into sublethally irradiated *TCR$\beta\delta$*-deficient recipient mice. As in heterozygous *Foxp3*$^{+/-}$ female mice, the presence of *Foxp3*$^+$ bone marrow-derived cells rescues the lymphoproliferative autoimmune syndrome (Fontenot et al., 2003). In this setting, functional responses of naive T cells derived from *Foxp3*$^+$ and *Foxp3*$^-$ bone marrow, as distinguished by expression of CD45.1, can be directly tested in the same mouse. Mixed bone marrow chimeric mice were infected with LCMV or ovalbumin-expressing L.m. (rLmOva) 8–12 weeks post-bone marrow reconstitution, and antigen-specific responses of both CD4$^+$ and CD8$^+$ T cells were assessed on day 7 and 8 postinfection by measuring intracellular cytokine production in response to in vitro restimulation with MHC class I- and MHC class II-restricted antigenic peptides. Prior to infection, peripheral blood was analyzed by flow cytometry to determine the relative contribution of the *Foxp3*$^-$ CD45.1$^-$ and *Foxp3*$^+$ CD45.1$^+$ bone marrow to the total T cell pool in each mouse. After infection with either LCMV or rLmOva, the relative percentages of *Foxp3*$^+$ and *Foxp3*$^-$ T cells remained constant. Furthermore, upon in vitro restimulation, *Foxp3*$^-$ and *Fopx3*$^+$ CD4$^+$ T cells (Figures 5B and 5C) and CD8$^+$ T cells (data not shown) produced IL-2, TNF-α, and IFN-γ with the same frequency and at the same levels on a per cell basis. Together, these data argue against a cell-intrinsic role for Foxp3 in regulating the expansion and cytokine production of nonregulatory T cells.

"Adaptive" Foxp3-Expressing T_R Cells Are Not Generated De Novo in the Course of Acute Immune Responses

Early studies suggested that antigen-driven differentiation of precursor T cells may result in de novo genera-

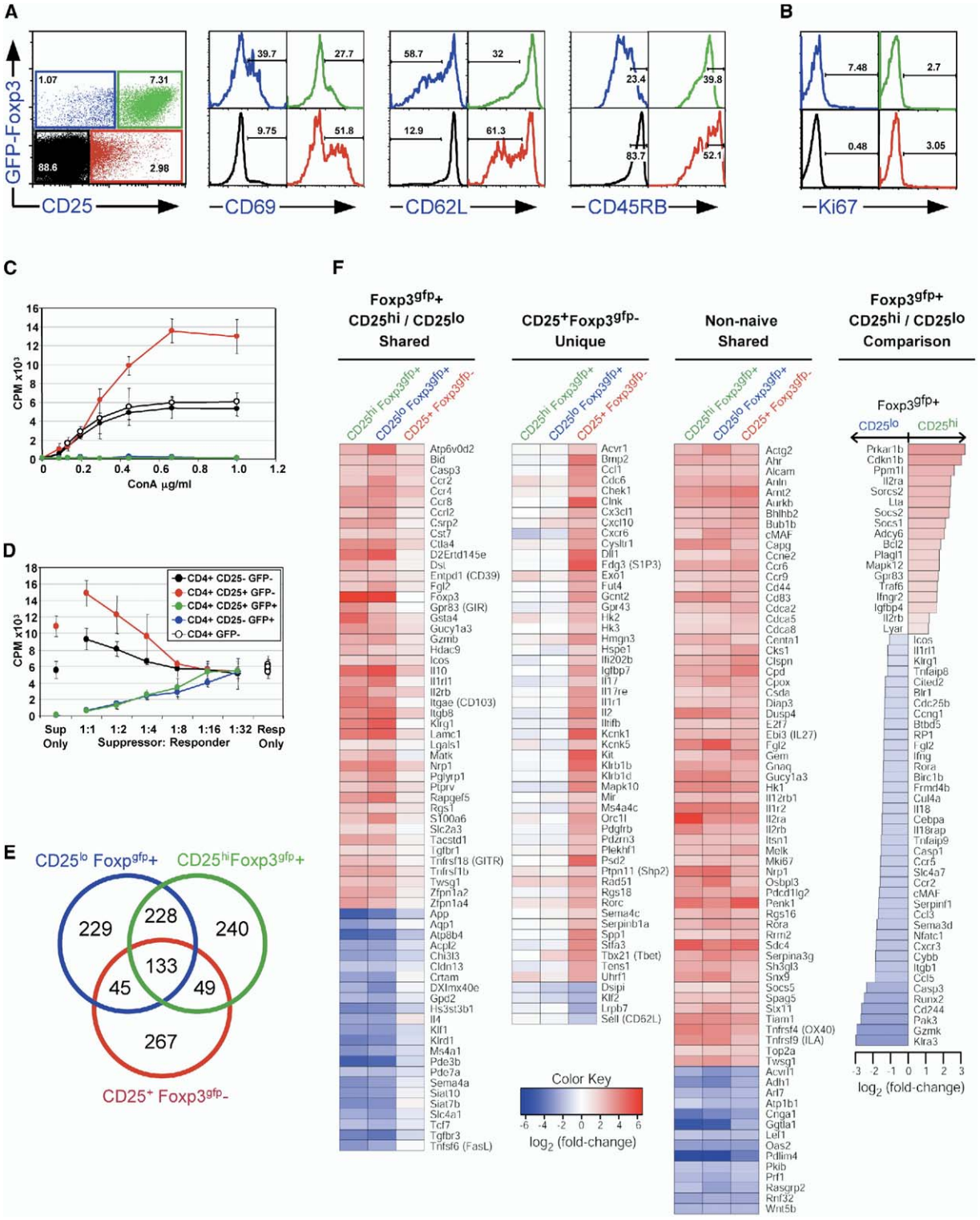

Figure 4. T_R Cell Phenotype and Function Correlates with Foxp3 Expression

(A) Flow cytometric analysis of Foxp3/CD25-expressing subpopulations of lymph node CD4+ cells. Histograms are shown for cells from each of the subpopulations as indicated in the first FACS plot (left panel) and correspond to the gated population of the same color and position in the first plot (CD25^{lo}Foxp3^{gfp+}, blue; CD25^{hi}Foxp3^{gfp+}, green; CD25^{+}Foxp3^{gfp-}, red; CD25^{-}Foxp3^{gfp-}, black).

(B) Flow cytometric identification of proliferating Ki67+ cells within Foxp3/CD25-expressing subpopulations of lymph node CD4+ T cells. Color-coded gates for four cell subsets are the same as above.

(C) In vitro proliferative responses of the indicated purified Foxp3/CD25-expressing CD4+ T cell subpopulations (1 × 10^4 cells/well) from

tion of antigen-specific suppressor T cells (Tandon et al., 1979). This would imply that a dominant suppression mechanism, i.e., Foxp3, is induced as feedback regulation to limit conventional antigen-specific immune responses. To address this issue, $CD4^+Foxp3^{gfp-}$ T cells from OT-II TCR transgenic *Foxp3*^{gfp} mice were FACS sorted to >99.8% purity and stimulated either in vitro in the presence of the Ova peptide and irradiated APCs, or in vivo by adoptive transfer into unirradiated $CD45.1^+$ congenic recipients followed by infection with rLmOva.

FACS analysis of OT-II $CD4^+$ T cells activated in vitro by titrated amounts of Ova peptide for various periods from 12 hr to 7 days revealed no detectable Foxp3 upregulation at any time point (Figure 5D and data not shown). Similarly, no Foxp3 expression was detected in adoptively transferred OT-II $CD4^+$ T cells 7 days postinfection with rLmOva (Figure 5D). In these experiments, antigen-specific activation of the adoptively transferred OT-II *Foxp3*^{gfp} T cells was confirmed by their expansion and cell surface expression of characteristic activation markers (CD25, CD69, CD62L) in rLmOva-infected, but not in wt L.m.-infected or uninfected recipient mice (Figure 5D and data not shown). These data do not rule out the possibility that under certain conditions some T cells can upregulate Foxp3. However, our experiments demonstrate that de novo generation of "adaptive" T_R cells by Foxp3 induction in nonregulatory T cells does not occur in the course of acute pathogen-driven immune responses.

T Cell-Specific Ablation of Foxp3

The dramatic difference in the phenotype of Foxp3-deficient mice when compared to mice depleted of $CD25^+$ cells (McHugh and Shevach, 2002; Taguchi and Takahashi, 1996) or lymphopenic mice reconstituted with $CD25^-$ T cells (Sakaguchi et al., 1995) suggested that Foxp3 may have immunoregulatory functions outside the T cell compartment or, perhaps, the hematopoietic system. While the lymphoproliferative autoimmunity observed in Foxp3-deficient mice can be ameliorated in the short term by neonatal transfer of $CD4^+CD25^+$ T_R cells (Fontenot et al., 2003), this result only demonstrates the remarkable immunosuppressive potential of $CD4^+CD25^+$ T_R cells, but does not prove a unique function for Foxp3 within this cell type. This fact is highlighted by the ability of $CD4^+CD25^+$ T_R cells to suppress immune pathology not resulting from $CD4^+CD25^+$ T_R cell defects such as in allograft transplantation (Wood and Sakaguchi, 2003). Although we have not observed expression of Foxp3 in non-T cells, this negative result does not exclude the possibility that a deficiency in Foxp3 expression in other cell types may contribute to the aggressive lymphoproliferative syndrome of Foxp3-deficient mice.

To directly resolve this major outstanding issue, we generated mice in which Foxp3 was deleted specifically in $\alpha\beta$ T cells by crossing mice harboring a loxP-flanked Foxp3 allele (Fontenot et al., 2003) to CD4-Cre transgenic mice (Wolfer et al., 2001). Consistent with a unique role for Foxp3 in T cells, male CD4-Cre *Foxp3*^{lox} mice develop the outward symptoms of Foxp3 deficiency, including runting and severe exfoliative dermatitis with the exact same kinetics and severity as age-matched *Foxp3*$^-$ mice. At day 14 of age, lymphoproliferation, as evidenced by total lymph node cellularity, was equivalent in CD4-Cre *Foxp3*^{lox} and *Foxp3*$^-$ mice (Figure 6A). Furthermore, $CD4^+$ T cells from mice of both genotypes contained equivalent proportions of cells expressing a panel of activation markers, including CD69, CD62L, CD25, and CD44 (Figure 6B). Thus, T cell-specific ablation of Foxp3 results in a lymphoproliferative autoimmune syndrome identical to that observed in $Foxp3^-$ mice.

TCR/MHC Interactions Drive T_R Cell Development

The signals driving T_R cell development in the thymus have not been defined. The data presented thus far argue that Foxp3 functions as the lineage specification factor for T_R cells. Thus, understanding the signals that induce Foxp3 expression in the thymus should illuminate the process by which this cell fate choice is made. Analysis of the $Foxp3^{gfp+}$ thymocytes revealed that Foxp3 expression was largely restricted to CD4 SP thymocytes (~83% of $Foxp3^{gfp+}$ thymocytes) (Figure 7A). However, minor populations of CD8 SP, DP, and DN cells were also evident. These populations of $Foxp3^{gfp+}$ cells expressed equivalent levels of TCR (data not shown). To assess the maturation stage of Foxp3-expressing thymocytes, we analyzed CD24, or heat-stable antigen (HSA), expression. CD24 is downregulated on mature SP thymocytes after transition from the

Foxp3^{gfp} mice cultured in the presence of Con A and irradiated *TCR*$\beta\delta^{-/-}$ splenocytes (4×10^4 cells/well) as APCs. ($CD25^{lo}Foxp3^{gfp+}$, blue; $CD25^{hi}Foxp3^{gfp+}$, green; $CD25^+Foxp3^{gfp-}$, red; $CD25^-Foxp3^{gfp-}$, black; see Figure 4D legend). A representative of three experiments is shown. (D) Foxp3 expression defines regulatory T cells within both $CD25^{hi}$ and $CD25^{lo}$ CD4 T cell subsets. An in vitro suppression assay was performed by using Con A stimulation of cocultures of 1×10^4 $Foxp3^{gfp-}$ T cells as responders, 4×10^4 irradiated *TCR*$\beta\delta^{-/-}$ splenocytes as APCs, and titrated numbers of indicated populations of purified Foxp3/CD25-expressing $CD4^+$ T cells from *Foxp3*^{gfp} mice as suppressors starting at a 1×10^4 cells/well. Data in (C) and (D) are presented as mean cpm ^{3}H-thymidine incorporation in triplicate cultures. Error bars indicate standard deviation of the mean.

(E and F) Comparison of gene expression profiles between four subsets of Foxp3/CD25-expressing $CD4^+$ T cells from *Foxp3*^{gfp} mice. (E) Overlap among gene lists generated by microarray expression profiling of each of the four FACS-sorted, Foxp3/CD25-expressing $CD4^+$ subpopulations described above. Differentially expressed genes were selected by comparing each of the indicated populations against the $CD4^+CD25^-Foxp3^{gfp-}$ population as described in the Experimental Procedures. The Venn diagram illustrates the number of genes shared between the three lists. (F) Curated heatmaps of distinct expression profiles revealed by microarray analysis of the four Foxp3/CD25 $CD4^+$ subpopulations. The genes for the first heatmap were selected from the 228 overlapping genes between the two Foxp3-expressing populations; for the second heatmap, genes were selected from the 267 genes unique to the $CD25^+$ $Foxp3^{gfp-}$ population; and for the third heatmap, genes were selected from the 133 genes differentially expressed by all three non-naive populations. Colors indicate $\log_2$ fold-change versus the baseline $CD25^-Foxp3^{gfp-}$ population. The rightmost panel illustrates differences in the mRNA expression profiles of the two Foxp3-expressing populations. For all four panels, genes were selected from the gene sets indicated in Figure 4E.

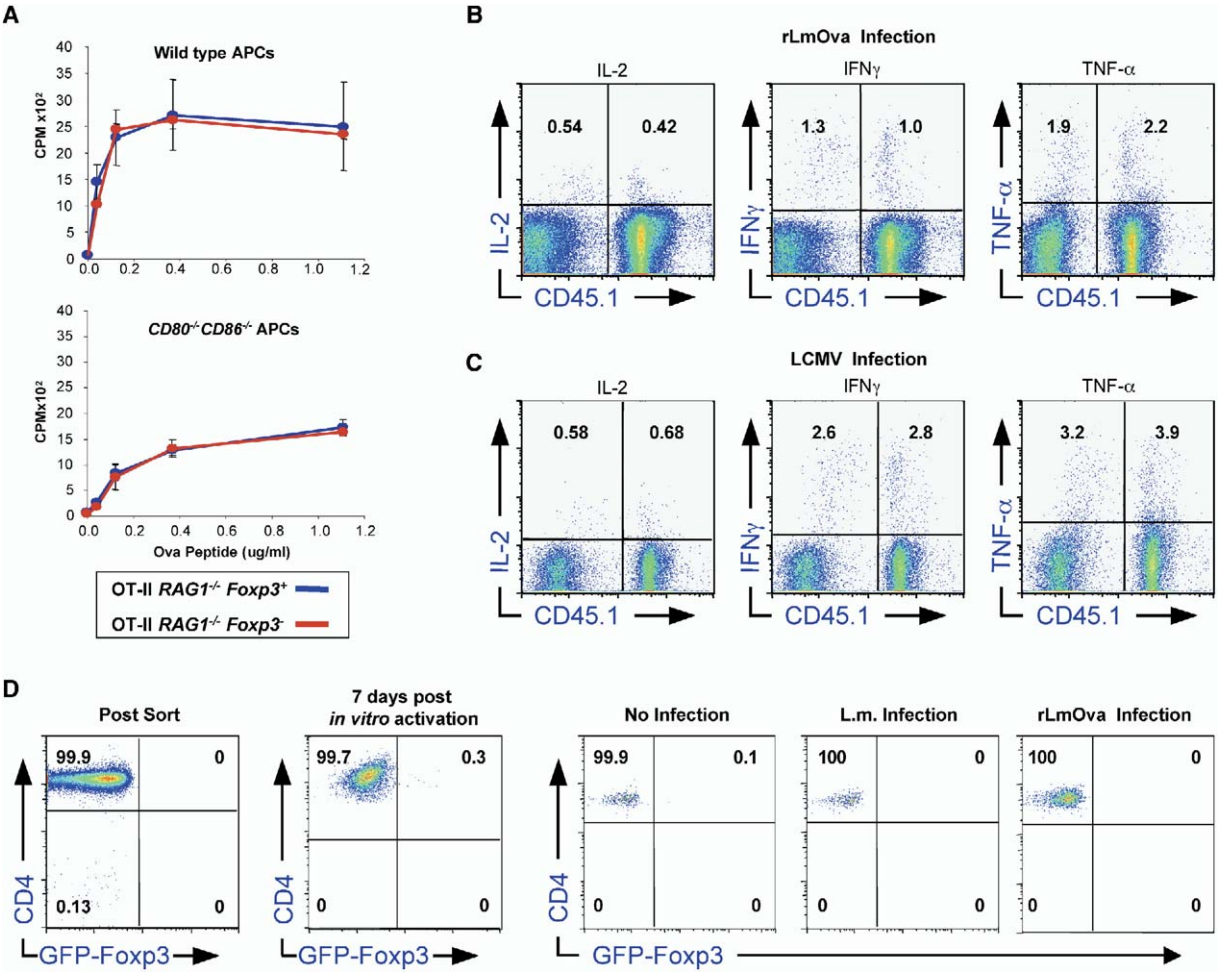

Figure 5. Lack of a Detectable Cell-Intrinsic Role for Foxp3 in Control of Nonregulatory CD4+ T Cells

(A) Foxp3 deficiency does not affect proliferative responses of naive CD4+ T cells. Proliferative responses of 2 × 10^4 CD4+ T cells from OT-II *RAG1*$^{-/-}$*Foxp3*$^{-}$ or *Foxp3*$^{+}$ mice to titrated amounts of Ova peptide in the presence of 4 × 10^4 irradiated CD11c+ Flt3L-induced wt or *CD80*$^{-/-}$*CD86*$^{-/-}$ dendritic cells. Data are presented as mean cpm ^{3}H-thymidine incorporation in triplicate cultures. Error bars indicate standard deviation of the mean.

(B and C) Comparable cytokine production by pathogen-specific *Foxp3*$^{+}$ (CD45.1+) or *Foxp3*$^{-}$ (CD45.1^{-}) CD4+ T cells from mixed bone marrow chimeras. Intracellular staining for indicated cytokines after (B) in vitro restimulation with LLO190-201 peptide of splenocytes isolated from mice 7 days after rLmOva infection and (C) in vitro restimulation with GP66 peptide of splenocytes isolated from mice 8 days after LCMV infection. Representative FACS plots of three or more mice per group are gated on CD4+ T cells. One of two similar experiments is shown.

(D) Lack of antigen-driven Foxp3 upregulation in nonregulatory CD4+ T cells upon antigenic challenge in vitro and in vivo. The leftmost panel shows representative flow cytometric analysis of Foxp3^{gfp-}CD4+ T cells sorted from OT-II *Foxp3*^{gfp} mice prior to activation in vitro or in vivo. The panel second from the left shows analysis of transferred T cells on day 7 of in vitro activation in the presence of CD45.1+ dendritic cells and Ova peptide. The last three panels show transferred T cells 8 days after infection of CD45.1+ host mice with indicated pathogen. Mice were infected 2 days after i.v. transfer of purified T cells. The gates for donor CD45.1^{-} cells are shown.

DP stage. Analysis of the CD24^{lo}Foxp3^{gfp+} population revealed a substantial decrease in the percentage of Foxp3^{gfp+}DP^{hi} cells but no significant change in CD4 SP, CD8 SP, DP^{dull}, or DN populations when compared to total Foxp3^{gfp+} cells (Figures 7A and 7B). Consistent with the low level of CD24 expression by the majority of Foxp3-expressing thymocytes, immunohistochemical analysis revealed that the majority of Foxp3^{gfp+} cells are found in the thymic medulla, the site known to harbor the most mature thymocyte population (Figure 7C). The few Foxp3^{gfp+} cells within the thymic cortex were in proximity to the cortico-medullary junction.

To more clearly delineate the relationship between thymic populations of Foxp3-expressing cells and to investigate a role for TCR signaling in Foxp3 induction, we crossed *Foxp3*^{gfp} mice on to MHC class I-deficient ($\beta_2M^{-/-}$), MHC class II-deficient ($A\beta^{b\ -/-}$), and double-deficient backgrounds ($\beta_2M^{-/-}A\beta^{b\ -/-}$). Analysis of $\beta_2M^{-/-}$*Foxp3*^{gfp} mice clearly demonstrates the dependence of the DP^{dull} and CD8 SP Foxp3^{gfp+} populations on MHC class I expression (Figures 7A and 7B). Likewise, development of the CD4 SP population is contingent upon MHC class II expression. No compensatory increase in the absolute numbers of CD8 SP Foxp3^{gfp+}

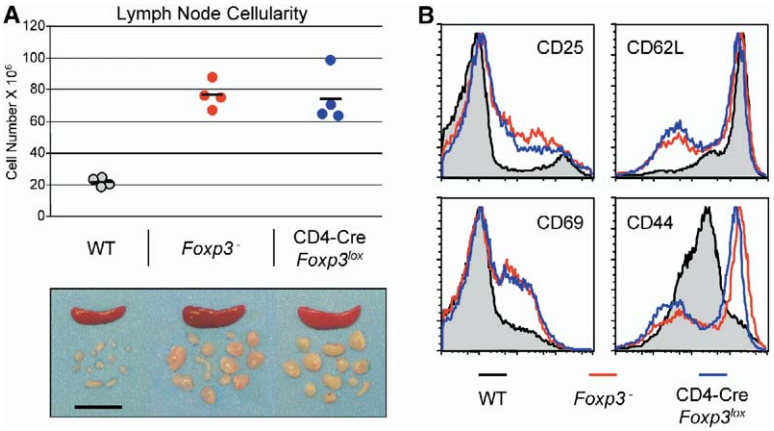

Figure 6. T Cell-Specific Deletion of Foxp3 Recapitulates the Lymphoproliferative Autoimmune Syndrome of Germline Foxp3-Deficient Mice

(A) Lymph node cellularity of 14-day-old wt, *Foxp3*$^{-}$, and CD4-Cre *Foxp3*^{lox} mice and photographs of lymph nodes and spleen from these mice.

(B) Expression of activation markers on CD4^{+} T cells in 14-day-old wt, *Foxp3*$^{-}$, and CD4-Cre *Foxp3*^{lox} mice. Representative flow cytometric data gated on CD4^{+} TCRβ^{+} cells are shown.

thymocytes was observed in MHC class II-deficient mice relative to wt mice (data not shown). Remarkably, Foxp3 expression was completely lost in all thymocytes, including expression in both the DN and immature CD24^{hi} DP populations, in $\beta_2M^{-/-}A\beta^{b\,-/-}$ double-deficient mice. These results identify both MHC class I- and MHC class II-restricted populations of Foxp3-expressing T cells developing in the thymus. Furthermore, they demonstrate that Foxp3 expression is independent of commitment to either the CD4 or CD8 lineage but strictly dependent on TCR/MHC interactions.

Discussion

We have recently demonstrated that Foxp3 is required for the thymic development of CD4^{+}CD25^{+} T_R cells (Fontenot et al., 2003). Ectopic expression of Foxp3 has also been shown to confer suppressor activity on some nonregulatory T cells (Fontenot et al., 2003; Hori et al., 2003; Khattri et al., 2003). While these data clearly demonstrate that Foxp3 has a critical role in CD4^{+}CD25^{+} T_R cell biology, it was unclear if this role was sufficient to explain the phenotype associated with Foxp3 deficiency. Foxp3 has been suggested to function as a negative regulator of T cell activation and, perhaps, as a transcriptional "effector" of an anti-inflammatory cytokine program (Clark et al., 1999; Khattri et al., 2001; Schubert et al., 2001). Thus, a reasonable hypothesis was that Foxp3 may play a common role in multiple cell types both within and, perhaps, outside the immune system to regulate immune activation and inflammation. Together, these roles could explain the aggressive life-threatening lymphoproliferation resulting from Foxp3 deficiency in both humans and mice. An alternative hypothesis would envision a unique role for Foxp3 in T_R cell lineage specification. In this scenario, Foxp3 expression is not limited to CD4^{+}CD25^{+} T cells. This im-

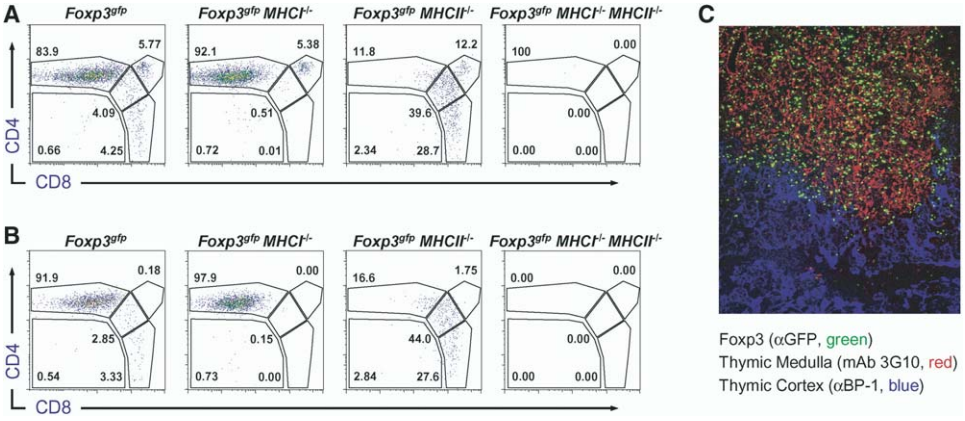

Figure 7. Thymic Development of Foxp3^{+} T_R Cells

(A) MHC class I- and MHC class II-restricted Foxp3-expressing thymocyte populations. Flow cytometric analysis of Foxp3^{gfp+} thymocytes from Foxp3^{gfp} mice on wt and MHC-deficient backgrounds. Plots are gated on total Foxp3^{gfp+} live cells from *Foxp3*^{gfp} mice of the indicated genotypes.

(B) Flow cytometric analysis of mature CD24^{lo}Foxp3^{gfp+} thymocyte subsets from *Foxp3*^{gfp} mice on wt and MHC-deficient backgrounds.

(C) Localization of Foxp3-expressing T_R cell precursors within the thymus. A representative immunostained thymic section from a *Foxp3*^{gfp} mouse is shown; Foxp3^{gfp+} thymocytes (αGFP, green); thymic cortex (αBP-1, blue); thymic medulla (mAb 3G10, red).

plies that deficiency in Foxp3 would result in complete loss of the T_R cell lineage and loss of the genetic mechanism of dominant tolerance.

Foxp3 as the T_R Cell Lineage Specification Factor

Our studies demonstrate that Foxp3 expression in αβ T cells, irrespective of CD25 expression, correlates with suppressor activity. Foxp3 expression is limited to a small subset of αβ T cells in both naive and pathogen-challenged animals. Moreover, Foxp3 deficiency does not impact the functional responses of nonregulatory T cells to biologically relevant antigens, i.e. pathogens, and induction of Foxp3 expression in nonregulatory T cells does not appear to be part of a pathogen-induced mechanism for limiting immune responses in vivo. We also show that Foxp3-expressing $CD4^+$ T cells share a common gene expression profile. While we have not been able to test the suppressive properties of the minor $CD8^+$, $CD4^+CD8^+$, and $CD4^-CD8^-$ $Foxp3^+$ T cell subsets due to very limited cell numbers, elevated cell surface expression of CD25, CTLA-4, and GITR on these cells is consistent with these cells having similar functional properties as $CD4^+Foxp3^+$ T cells (Figure S3). Thus, we believe that the preponderance of evidence is consistent with all Foxp3-expressing cells being part of the T_R cell population. In aggregate, these data argue that Foxp3 functions as the T_R cell lineage specification factor.

The remarkably restricted expression of Foxp3 to a subset of αβ T cells, as revealed in our analysis, is highly unusual for a transcription factor and suggests a recent evolutionary origin. Although a role for Foxp3 in nonhematopoietic cells has been suggested to contribute to the aggressive lymphoproliferative syndrome observed in Foxp3-deficient mice, we have found no evidence of Foxp3 expression in nonhematopoietic tissues. More importantly, it is clear that T cell-specific deletion of Foxp3 is sufficient to induce the identical lymphoproliferative syndrome observed in mice with germline Foxp3 deficiency. This result establishes a vital role for Foxp3-expressing T_R cells in the maintenance of dominant tolerance to self. Moreover, it unequivocally demonstrates a deficiency in T_R cells as the cause of the fatal IPEX autoimmune syndrome in humans and its correlate in mice.

$CD25^{lo}Foxp3^+$ Regulatory T Cells

Our analysis of the total CD4 population of the *Foxp3^{gfp}* mice revealed two intriguing populations: regulatory $CD4^+CD25^{lo}Foxp3^{gfp+}$ T cells and activated/effector $CD4^+CD25^+Foxp3^{gfp-}$ T cells. The nature of the regulatory $CD4^+CD25^{lo}Foxp3^{gfp+}$ T cell population is of particular interest. The importance of this population is underscored by the fact that these cells comprise greater than 50% of the tissue-infiltrating, Foxp3-expressing T cell population in the lungs of both uninfected and M.tb.-infected *Foxp3^{gfp}* mice. These data highlight the limitations of using CD25 as a marker for T_R cells. Notably, the $CD4^+CD25^{lo}Foxp3^{gfp+}$ T cell population is enriched for cells with an activated surface phenotype and for proliferating cells. Consistent with these findings, comparisons of the transcriptional profiles of $CD4^+CD25^{lo}Foxp3^{gfp+}$ T cells and $CD4^+CD25^{hi}Foxp3^{gfp+}$ T cells showed upregulation of a number of genes responsible for regulatory effector function or tissue migration such as ICOS, IL-10, CCR2, CXCR3, CCR5, and β1-integrin in the $CD25^{lo}$ population.

Despite low surface levels of CD25, these cells express elevated levels of both CD25 (IL-2Rα) and CD122 (IL-2Rβ) mRNA, albeit lower than $CD4^+CD25^{hi}Foxp3^{gfp+}$ T cells. It is likely that a portion of these cells has transiently downregulated CD25 upon proliferation, as decreased levels of CD25 on T_R cells undergoing homeostatic proliferation have been previously reported (Gavin et al., 2002). CD25 downregulation may also result from trafficking to areas where IL-2 is limiting, as maintenance of CD25 expression in $Foxp3^+$ T_R cells is IL-2 dependent (J.D.F. and A.Y.R., unpublished data). The increase in this population in the secondary lymphoid organs and peripheral tissues is consistent with this phenotype developing in the periphery upon activation or upon IL-2 deprivation of $CD4^+CD25^{hi}Foxp3^{gfp+}$ T cells. Importantly, our data demonstrate that $CD4^+CD25^{lo}Foxp3^{gfp+}$ T cells maintain potent suppressive activity. Consistent with these results, analysis of $CD4^+$ T cells from the lung and draining lymph node of M.tb.-infected mice demonstrate that only the $Foxp3^{gfp-}$, but none of the $Foxp3^{gfp+}$ cells, produce proinflammatory cytokines such as TNF-α or IFN-γ (data not shown).

Activated/Effector $CD4^+CD25^+Foxp3^-$ T Cells

We have also identified a population of $CD4^+CD25^+$ $Foxp3^{gfp-}$ T cells. These cells are highly enriched for activated/effector cells as suggested by their transcriptional profile demonstrating upregulation of cytokine or cytokine regulation-related genes (e.g., IL-2, IL-4, T-bet), as well as genes related to cell cycle and apoptosis. FACS analysis confirmed the activated phenotype of $CD4^+CD25^+Foxp3^{gfp-}$ T cells. Furthermore, $CD4^+CD25^+$ $Foxp3^{gfp-}$ T cells exhibit a remarkably high proliferative potential in vitro and were significantly increased in numbers in the spleen, draining lymph nodes, and lung of M.tb.-infected mice (data not shown). These results suggest that, in normal mice, this subset contains T cells responding to microbial or autoantigens. These results again highlight the utility of Foxp3 in distinguishing T_R from the activated/effector cells within the $CD25^+$ T cell population, especially in settings of immune activation.

Signals Required for Induction of Foxp3 in the Thymus

What are the signals that induce Foxp3 expression and T_R cell lineage commitment? In agreement with their mature phenotype, we find the vast majority of Foxp3-expressing thymocytes localized to the medulla, with the remaining $Foxp3^+$ cells located in the deep cortex, adjacent to the cortico-medullary junction. These latter cells most likely correspond to the subset of immature $CD24^{hi}Foxp3^{gfp+}$ DP thymocytes. Foxp3-expressing SP and DP subsets appear concurrently during mouse development and in fetal thymic organ culture (J.D.F. and A.Y.R., unpublished data). Thus, we find no evidence

for a precursor-product relationship between the CD24^{hi}Foxp3^{gfp+} DP population and the CD24^{lo} Foxp3^{gfp+} populations. Furthermore, the highly diverse TCR repertoire of the CD4$^+$CD25$^+$ T_R cell population argues against such a scenario (Hsieh et al., 2004; Takahashi et al., 1998).

Our analysis of MHC-deficient ($\beta_2M^{-/-}A\beta^{b\,-/-}$) *Foxp3^{gfp}* mice demonstrates that TCR/MHC interactions are required for induction of Foxp3 expression. We observed Foxp3 expression in immature CD24^{hi} DP thymocytes in MHC class I-deficient, and MHC class II-deficient, as well as wt backgrounds and an absolute MHC dependence for Foxp3 upregulation in these populations. These data argue that Foxp3 expression does not require transition to the SP stage and that DP thymocytes rely on TCR interactions with either MHC class I or MHC class II for Foxp3 induction. These observations are consistent with an instructive role for TCR signaling in induction of Foxp3 expression and, therefore, T_R cell development. Furthermore, these data rule out a stochastic/selective model in which DP thymocytes randomly upregulate Foxp3 prior to positive selection, since this model predicts the presence of Foxp3-expressing DP thymocytes in a MHC-deficient setting.

The unexpected presence of both MHC class I- and MHC class II-restricted Foxp3-expressing cell populations also demonstrates that Foxp3 expression does not depend on specific CD4 or CD8 lineage choice. However, the fact that the great majority of Foxp3-expressing thymocytes are MHC class II-restricted CD4 SP suggests that the signals driving the CD4/CD8 lineage choice may also be linked to Foxp3 induction. One possible explanation for the prevalence of Foxp3-expressing CD4 SP is offered by the view that CD4 lineage commitment requires a TCR signal of a greater strength or extended duration than that needed for CD8 lineage commitment (Bosselut, 2004). Notably, recent studies from our lab suggest that a large number of CD25$^+$CD4$^+$ T_R cells express TCRs with an increased avidity for self-peptide-MHC complexes (Hsieh et al., 2004). Together with observations that coexpression of transgenes encoding a TCR and its cognate ligand can promote the development of CD4$^+$CD25$^+$ T_R cells (Apostolou et al., 2002; Jordan et al., 2001), these results argue that the TCR avidity of the bulk of T_R cells is likely to fall within the grey area between positive and negative selection, and would allow for stronger and/or more persistent TCR signal resulting in the prevalent development of CD4 lineage cells expressing Foxp3.

In conclusion, data presented herein argue that Foxp3 acts as the T_R cell lineage specification factor and mediator of the genetic mechanism of dominant tolerance. Based on these data, we propose that Foxp3 expression defines the T_R cell lineage. The fatal autoimmune disease observed in mice with T cell-specific ablation of Foxp3 demonstrates T_R cell-mediated dominant tolerance to be a vital mechanism of immune homeostasis. We suggest that the need for such a dedicated mechanism was driven by the emergence of MHC-restricted recognition by T cells and the associated developmental requirements for reactivity with self-peptide-MHC complexes. The early onset of the lymphoproliferative syndrome in mice deficient in Foxp3, and thus T_R cells, suggests that this mechanism evolved to control T cell self-reactivity and autoimmune inflammation. As a consequence of this function, T_R cells cause downmodulation of chronic inflammation associated with other types of immune responses while not specifically developing to limit pathogen-specific responses. Finally, the absolute dependence of Foxp3 expression on TCR-peptide-MHC interactions in the thymus strongly argues that dominant tolerance is not a hard-wired, but an induced, mechanism of negative feedback regulation to maintain immune homeostasis through recognition of molecular self.

Experimental Procedures

Mice

Mice were housed under specific pathogen-free conditions and used according to the guidelines of the Institutional Animal Care Committee at the University of Washington. Generation of the *Foxp3^{gfp}* allele is described in Figure S1. *Foxp3$^-$* and *Foxp3^{lox}* were previously described (Fontenot et al., 2003). C57BL/6, B6.SJL-*Ptprc^a Pep3^b*/BoyJ, and C57BL/6J-*Rag1^{tm1Mom}* and TCR$\beta\delta^{-/-}$ mice were from the Jackson Laboratory (Bar Harbor, ME). Additional previously described mouse lines used in these studies include: OT-II TCR, CD4-Cre, $\beta_2M^{-/-}$, *Ab$\beta^{-/-}$*, and *CD80$^{-/-}$CD86$^{-/}$*. All mice were used at the age of 6–12 weeks unless specified in the text.

Antibodies, FACS Analysis, and Cell Sorting

Conjugated antibodies were purchased from both BD Pharmingen (San Jose, CA) and eBioscience (San Diego, CA). FACS analysis was preformed by using FACSCalibur and LSR II flow cytometers (Becton Dickinson, Palo Alto, CA) and were analyzed with FlowJo software.

For analysis of CD4$^+$CD25 × Foxp3^{gfp} subsets, CD4$^+$ T cells were enriched prior to FACS sorting by depletion of total lymph node and spleen cell suspension with a cocktail of biotinylated antibodies specific for CD8, B220, CD11b, NK1.1, and DX5, followed by anti-biotin MACS beads. The remaining cells were labeled with CD4-PerCP antibodies, CD25-APC antibodies, and PE-conjugated streptavidin. CD4$^+$PE$^-$ cells were sorted into four populations based on expression of GFP and CD25 as indicated in Figure 5 to greater than 90% purity. All cell sorting was performed by using the FACSAria cell sorter.

T Cell Functional Assays

Proliferation and suppression assays were preformed as described, with modifications as indicated in the figure legends (Fontenot et al., 2003). In Figure 2, suppressor cells were MACS purified by using PC61 antibody. In some experiments, OT-II T cells were stimulated with titrated amounts of ovalbumin 323–339 peptide in the presence of irradiated, MACS-purified, CD11c$^+$ FLT3L-induced dendritic cells prepared as described (Mach et al., 2000). All data are shown as mean [^{3}H]thymidine incorporation in triplicate cultures. Error bars indicate standard deviation of the mean.

For analysis of pathogen-specific immune responses, infections, T cell stimulation, and intracellular cytokine staining of splenic T cell populations isolated from Lm-, rLmOva-, or LCMV-infected mice were conducted as previously described (Tyznik et al., 2004).

Microarray Sample Preparation and Analysis

Total RNA was isolated by using the RNeasy Mini Kit (Qiagen). Biotinylated antisense cRNA was prepared by using two cycles of in vitro amplification according to the Affymetrix Small Sample Labeling Protocol II. 15 μg biotinylated cRNA was fragmented and hybridized to Affymetrix GeneChip Mouse Genome 430 2.0 arrays at the Stanford PAN Facility (Palo Alto, CA).

All data analyses were performed by using Bioconductor version 1.5 (Gentleman et al., 2004) for the statistical software R (http://www.r-project.org). Expression values were background corrected,

normalized, and summarized by using the default settings of the *gcrma* package (Wu et al., 2004). As these values exhibited intensity-dependent variation, we used a sliding intensity window to select differentially expressed genes for each pairwise comparison. Within each slice along the intensity scale, probe sets with a fold-change $\geq$ 2.57 standard deviations away from the local mean and a minimum average $\log_2$ average intensity value of 4 were selected. Heatmaps were generated by hand curation of these gene lists.

Microscopy and Immunohistochemistry

For single-cell imaging, purified $CD4^+CD25^+$ T cells were fixed with 4% paraformaldehyde in PBS prior to deposition on poly-L-lysine-coated slides by cytospin. Direct GFP fluorescence and DAPI counterstain were imaged with an API-Delta Vision deconvolution microscopy system. Thymic sections were prepared and stained as described (Lehar et al., 2004) with rabbit anti-GFP antibody, digoxigenin-conjugated mAb 3G10, and Alexa-647-conjugated anti-BP1(6C3); followed by Alexa 546-conjugated goat anti-rabbit IgG, anti-digoxigenin-fluorescein; followed by Alexa 488-conjugated rabbit anti-fluorescein. Images were acquired with a Leica SP1/MP confocal microscope.

Supplemental Data

Supplemental Data including four supplemental figures are available at http://www.immunity.com/cgi/content/full/22/3/329/DC1/.

Acknowledgments

We thank K. Forbush, P. deRoos, Y. Liang, C. Plata, and L. Karpik for technical expertise and mouse colony management and A. Tyznik and J. Sun for advice and assistance with infections. Additionally, we thank A. Gallegos, M. Gavin, K. Honey, and C. Hsieh for critical reading of the manuscript and all members of the Rudensky lab for thoughtful advice and provocative discussions. This work was supported by training grants from the National Institutes of Health (NIH) and the Cancer Research Institute (J.D.F.) and grants from the NIH (A.Y.R., A.G.F.). A.Y.R. is a Howard Hughes Medical Institute investigator.

Received: January 13, 2005
Revised: January 21, 2005
Accepted: January 26, 2005
Published: March 22, 2005

References

Apostolou, I., Sarukhan, A., Klein, L., and von Boehmer, H. (2002). Origin of regulatory T cells with known specificity for antigen. Nat. Immunol. *3*, 756–763.

Bosselut, R. (2004). CD4/CD8-lineage differentiation in the thymus: from nuclear effectors to membrane signals. Nat. Rev. Immunol. *4*, 529–540.

Brunkow, M.E., Jeffery, E.W., Hjerrild, K.A., Paeper, B., Clark, L.B., Yasayko, S.A., Wilkinson, J.E., Galas, D., Ziegler, S.F., and Ramsdell, F. (2001). Disruption of a new forkhead/winged-helix protein, scurfin, results in the fatal lymphoproliferative disorder of the scurfy mouse. Nat. Genet. *27*, 68–73.

Clark, L.B., Appleby, M.W., Brunkow, M.E., Wilkinson, J.E., Ziegler, S.F., and Ramsdell, F. (1999). Cellular and molecular characterization of the scurfy mouse mutant. J. Immunol. *162*, 2546–2554.

Fontenot, J.D., Gavin, M.A., and Rudensky, A.Y. (2003). Foxp3 programs the development and function of CD4+CD25+ regulatory T cells. Nat. Immunol. *4*, 330–336.

Gavin, M.A., Clarke, S.R., Negrou, E., Gallegos, A., and Rudensky, A. (2002). Homeostasis and anergy of CD4(+)CD25(+) suppressor T cells in vivo. Nat. Immunol. *3*, 33–41.

Gentleman, R.C., Carey, V.J., Bates, D.M., Bolstad, B., Dettling, M., Dudoit, S., Ellis, B., Gautier, L., Ge, Y., Gentry, J., et al. (2004). Bioconductor: open software development for computational biology and bioinformatics. Genome Biol. *5*, R80.

Godfrey, V.L., Wilkinson, J.E., and Russell, L.B. (1991). X-linked lymphoreticular disease in the scurfy (sf) mutant mouse. Am. J. Pathol. *138*, 1379–1387.

Hori, S., Nomura, T., and Sakaguchi, S. (2003). Control of regulatory T cell development by the transcription factor Foxp3. Science *299*, 1057–1061.

Hsieh, C.S., Liang, Y., Tyznik, A.J., Self, S.G., Liggitt, D., and Rudensky, A.Y. (2004). Recognition of the peripheral self by naturally arising CD25+ CD4+ T cell receptors. Immunity *21*, 267–277.

Jordan, M.S., Boesteanu, A., Reed, A.J., Petrone, A.L., Holenbeck, A.E., Lerman, M.A., Naji, A., and Caton, A.J. (2001). Thymic selection of CD4+CD25+ regulatory T cells induced by an agonist self-peptide. Nat. Immunol. *2*, 301–306.

Khattri, R., Kasprowicz, D., Cox, T., Mortrud, M., Appleby, M.W., Brunkow, M.E., Ziegler, S.F., and Ramsdell, F. (2001). The amount of scurfin protein determines peripheral T cell number and responsiveness. J. Immunol. *167*, 6312–6320.

Khattri, R., Cox, T., Yasayko, S.A., and Ramsdell, F. (2003). An essential role for Scurfin in CD4+CD25+ T regulatory cells. Nat. Immunol. *4*, 337–342.

Lehar, S.M., Dooley, J., Farr, A.G., and Bevan, M.J. (2004). Notch ligands Delta1 and Jagged1 transmit distinct signals to T cell precursors. Blood *105*, 1440–1447.

Mach, N., Gillessen, S., Wilson, S.B., Sheehan, C., Mihm, M., and Dranoff, G. (2000). Differences in dendritic cells stimulated in vivo by tumors engineered to secrete granulocyte-macrophage colony-stimulating factor or Flt3-ligand. Cancer Res. *60*, 3239–3246.

McHugh, R.S., and Shevach, E.M. (2002). Cutting edge: depletion of CD4+CD25+ regulatory T cells is necessary, but not sufficient, for induction of organ-specific autoimmune disease. J. Immunol. *168*, 5979–5983.

McHugh, R.S., Whitters, M.J., Piccirillo, C.A., Young, D.A., Shevach, E.M., Collins, M., and Byrne, M.C. (2002). CD4(+)CD25(+) immunoregulatory T cells: gene expression analysis reveals a functional role for the glucocorticoid-induced TNF receptor. Immunity *16*, 311–323.

Sakaguchi, S., Sakaguchi, N., Asano, M., Itoh, M., and Toda, M. (1995). Immunologic self-tolerance maintained by activated T cells expressing IL-2 receptor alpha-chains (CD25). Breakdown of a single mechanism of self-tolerance causes various autoimmune diseases. J. Immunol. *155*, 1151–1164.

Schubert, L.A., Jeffery, E., Zhang, Y., Ramsdell, F., and Ziegler, S.F. (2001). Scurfin (FOXP3) acts as a repressor of transcription and regulates T cell activation. J. Biol. Chem. *276*, 37672–37679.

Shevach, E.M. (2002). CD4+ CD25+ suppressor T cells: more questions than answers. Nat. Rev. Immunol. *2*, 389–400.

Taguchi, O., and Takahashi, T. (1996). Administration of anti-interleukin-2 receptor alpha antibody in vivo induces localized autoimmune disease. Eur. J. Immunol. *26*, 1608–1612.

Takahashi, T., Kuniyasu, Y., Toda, M., Sakaguchi, N., Itoh, M., Iwata, M., Shimizu, J., and Sakaguchi, S. (1998). Immunologic self-tolerance maintained by CD25+CD4+ naturally anergic and suppressive T cells: induction of autoimmune disease by breaking their anergic/suppressive state. Int. Immunol. *10*, 1969–1980.

Tandon, P., Chaturvedi, U.C., and Mathur, A. (1979). Dengue virus-induced thymus-derived suppressor cells in the spleen of mice. Immunology *38*, 653–658.

Tyznik, A.J., Sun, J.C., and Bevan, M.J. (2004). The CD8 population in CD4-deficient mice is heavily contaminated with MHC class II-restricted T cells. J. Exp. Med. *199*, 559–565.

Wolfer, A., Bakker, T., Wilson, A., Nicolas, M., Ioannidis, V., Littman,

D.R., Lee, P.P., Wilson, C.B., Held, W., MacDonald, H.R., and Radtke, F. (2001). Inactivation of Notch 1 in immature thymocytes does not perturb CD4 or CD8T cell development. Nat. Immunol. *2*, 235–241.

Wood, K.J., and Sakaguchi, S. (2003). Regulatory T cells in transplantation tolerance. Nat. Rev. Immunol. *3*, 199–210.

Wu, Z., Irizarry, R.A., Gentleman, R., Martinez-Murillo, F., and Spencer, F. (2004). A model based background adjustment for oligonucleotide expression arrays. Johns Hopkins University, Department of Biostatistics Working Papers, *Working Paper 1*, http://www.bepress.com/jhubiostat/paper1.

Zahorsky-Reeves, J.L., and Wilkinson, J.E. (2001). The murine mutation scurfy (sf) results in an antigen-dependent lymphoproliferative disease with altered T cell sensitivity. Eur. J. Immunol. *31*, 196–204.

Accession Numbers

The complete microarray data set has been deposited in the GEO database at NCBI (accession number GSE2389).